



HAL
open science

Soon Capturing and Frequency Analysis for Mesh Adaptive Interpolation

Bernadette Palmerio, Alain Dervieux

► **To cite this version:**

Bernadette Palmerio, Alain Dervieux. Soon Capturing and Frequency Analysis for Mesh Adaptive Interpolation. RR-2722, INRIA. 1995. inria-00073971

HAL Id: inria-00073971

<https://inria.hal.science/inria-00073971>

Submitted on 24 May 2006

HAL is a multi-disciplinary open access archive for the deposit and dissemination of scientific research documents, whether they are published or not. The documents may come from teaching and research institutions in France or abroad, or from public or private research centers.

L'archive ouverte pluridisciplinaire **HAL**, est destinée au dépôt et à la diffusion de documents scientifiques de niveau recherche, publiés ou non, émanant des établissements d'enseignement et de recherche français ou étrangers, des laboratoires publics ou privés.



INSTITUT NATIONAL DE RECHERCHE EN INFORMATIQUE ET EN AUTOMATIQUE

*Soon Capturing and Frequency
Analysis for Mesh Adaptive Interpolation*

Bernadette Palmerio - Alain Dervieux

N° 2722

Novembre 1995

PROGRAMME 6

*R*apport
de recherche

Les rapports de recherche de l'INRIA
sont disponibles en format postscript sous
ftp.inria.fr (192.93.2.54)

si vous n'avez pas d'accès ftp
la forme papier peut être commandée par mail :
e-mail : dif.gesdif@inria.fr
(n'oubliez pas de mentionner votre adresse postale).

par courrier :
Centre de Diffusion
INRIA
BP 105 - 78153 Le Chesnay Cedex (FRANCE)

INRIA research reports
are available in postscript format
ftp.inria.fr (192.93.2.54)

if you haven't access by ftp
we recommend ordering them by e-mail :
e-mail : dif.gesdif@inria.fr
(don't forget to mention your postal address).

by mail :
Centre de Diffusion
INRIA
BP 105 - 78153 Le Chesnay Cedex (FRANCE)

**SOON CAPTURING AND FREQUENCY
ANALYSIS FOR MESH ADAPTIVE
INTERPOLATION**

Bernadette PALMERIO
University of Nice and INRIA

Alain DERVIEUX
INRIA, BP 93, 2004 route des lucioles
06902 SOPHIA-ANTIPOLIS

SOON CAPTURING AND FREQUENCY ANALYSIS FOR MESH ADAPTIVE INTERPOLATION

Bernadette PALMERIO

Alain DERVIEUX

Abstract

Let us call a **highly heterogeneous function** a function that is either locally singular or a smooth function but, with too small details in comparison with domain size. We study the L^2 norm of the interpolation error E_h between a function u and $\Pi_h u$ its $P1$ continuous interpolate: we use four examples of functions, that represent different cases of **highly heterogeneous functions**. When a sequence of uniform meshes is chosen, if we examine the convergence of E_h as a function of number of nodes, we observe a convergence of order 2 for a smooth function and when the number of nodes large enough. Conversely, when an adaptive mesh sequence is applied, second-order convergence is almost always observed. We give some theoretical arguments concerning this phenomenon.

Following some ideas currently used in spectral methods, we consider the $P1$ approximation of u on nested meshes and express the representation of u_h as a series with increasing fineness of its terms. The size of each terms as a function of the corresponding level number is examined.

Keywords: Finite Elements, $P1$ Interpolation, convergence, mesh adaptive method, criterion, spring system.

CAPTURE ET ANALYSE FREQUENTIELLE POUR L'INTERPOLATION A PARTIR DE MAILLAGES ADAPTATIFS

Bernadette PALMERIO

Alain DERVIEUX

Résumé

Introduisons la notion de **fonction fortement hétérogène**: c'est une fonction, soit singulière, soit régulière mais avec des zones de rapides variations par rapport à la taille du domaine. On étudie le comportement de la norme L^2 de l'erreur d'interpolation E_h d'une fonction fortement hétérogène et de $\Pi_h u$ son interpolée $P1$. Cette étude est faite à partir de quatre fonctions tests fortement hétérogènes. En évaluant le comportement de l'erreur E_h en fonction du nombre de noeuds, on obtient une convergence à l'ordre 2, en maillage uniforme et pour une fonction régulière, seulement à partir du point où le nombre de noeuds est suffisant, et en maillage adapté beaucoup plus tôt. S'inspirant d'une méthode de l'approximation spectrale appliquée à l'interpolation $P1$ d'une fonction u sur des maillages emboîtés, on écrit une représentation de u_h sous la forme d'une série composée de termes de finesse décroissante. On étudie alors la norme de chaque terme en fonction du niveau de maillage. On déduit de cette "*analyse fréquentielle*" un critère pour les systèmes de maillages adaptatifs

Mots clefs: Elements finis, interpolation $P1$, convergence, méthodes de maillages adaptatifs.

1 Introduction

Mesh adaption is a technique that is more and more frequently studied and used in Computational Continuum Mechanics. While practical motivations for adapting the mesh are clear, theoretical formalizations of the advantage of this technique are yet rare.

The approximation theory aims at predicting the approximation error, or, at least, its asymptotic behavior when the mesh is made finer and finer. For example, the linear Galerkin finite element method is analysed as giving an error four times smaller with a mesh twice finer, as far as both meshes are fine enough.

This second-order accuracy statement cannot be improved by applying an adaptive version of this approximation scheme. So where is the bonus?

In this paper we examine two analyses aiming at characterizing the adaption bonus. They are presented within the most simplified context we found, dealing with one-dimensional Mesh-Adaptive Interpolation.

What do we call Mesh Adaptive Interpolation (“MAI”) ?

The problem addressed most frequently is the mesh adaptive research of the solution of a Partial Differential Equation (Mesh Adaptive Approximation, MAA):

$$MAA : Au = f ; \text{ find } \Pi_h u, \text{ discrete, near } u \quad (1)$$

Clearly, it is difficult to find the most efficient mesh to give a good discrete function representing a continuous one, u which we do not know !

In the case where $A \equiv Id$, we call this MAI :

$$MAI : u \text{ is known, find a discrete } \Pi_h u \text{ close to } u \quad (2)$$

In this formulation, $\Pi_h u$ has to be described by a bounded set of information : one mesh, a set of degrees of freedom.

This second type of problem is an important one : for example , when numerically solving a PDE, we generally build a mesh that is adapted to data and geometry. Another important application of MAI is **data compression** or **function tabulation** : the best way to represent a function with a small storage is likely not the approximation by a step function on an uniform mesh.

Why not use directly u ? $u(x)$ can be expensive to compute. $\Pi_h u(x)$ is less expensive as far as it easy to store the description of $\Pi_h u$ and

to compute $\Pi_h u$ from it; we shall roughly define the cost of $\Pi_h u$ as the number N of degrees of freedom used to represent $\Pi_h u$.

The next question is: **in what sense is $\Pi_h u$ observed as “close to u ” ?**

In theory, we are able to compute any (bounded) functional norm $\|\cdot\|$ of the error :

$$E_h = \|\Pi_h u - u\| = \textit{small} \quad (3)$$

but to compute it can be too costly, since handling $u(x)$ is expensive.

Thus we wish :

- (i) to find $\Pi_h u$, without using too much u
- (ii) to evaluate $|\Pi_h u - u|$ without using too much u .

A significant example is the following : each measure or computation of the lift u of a plane for a given angle of attack x can be as costly as 1 CRAY-night ; how to proceed in order to observe only a few x values and to rebuild the corresponding $u(x)$ (“polar”) curve ? How to evaluate the accuracy of this table ?

Let us now comment the relation between Problems (i) and (ii) : in Problem (i), we wish the best efficiency, that is, a good $\Pi_h u$ from a few values $u(x_i)$ or, more or less equivalently, from a coarse mesh ; one clever strategy could be to adapt progressively the mesh, from some measures of its effectiveness. Now, in Problem (ii), we investigate the different manners to measure the effectiveness of the mesh.

Let us come back to MAA: we consider the solution u of the Partial Differential Equation (1).

Let us call $\Pi_h u$ the solution of the corresponding discrete system. We call u a **highly heterogeneous solution** if it verifies:

- (C_1) either u is a smooth function, but its variation contains too small details in comparison with the usual uniform mesh size
- (C_2) either u is a singular function.

Some results concerning the approximation error

$$\varepsilon_h = \|u_h - u\| \quad (4)$$

in regular or in heterogeneous case are collected in Table 1

METHOD :	(1)REGULAR CASE	(2)HIGHLY HETEROG. CASE
SPECTRAL or H. ORD. CENT. DIFFER.	$\varepsilon = O(\frac{1}{N^\alpha}), 1 < \alpha < \infty$	Oscillations (Gibbs)
TVD, ENO (TVD: L^1 error)	$\varepsilon = O(\frac{1}{N^\alpha})$ $1 < \alpha < \infty$	$\varepsilon = O(\frac{1}{N})$

Table 1 : Behavior of the approximation error $\varepsilon_h = \|u_h - u\|$ when using several methods for the resolution of the discrete problem : N is the number of grid nodes. Two cases are considered: (1) regular function, (2) highly heterogeneous function, assuming that some details are too small for the mesh.

The contribution of this paper concerns two points.

For Problem (i), we propose a set of convergence properties that will enlight some typical advantages in using a class of mesh adaptive algorithms rather than using uniform mesh strategies.

For Problem (ii), we propose heuristics for evaluating whether a discrete solution $\Pi_h u$ is a good approximation of a continuous one or not, and how large may be the deviation $\Pi_h u - u$.

Before this, in order to be more precise, we shall define a simplified context :

Simplified context : P1-Galerkin, 1D

Let u a function defined on $[0, 1]$, bounded, piecewise continuous, with a finite number of discontinuities.

Let us consider a subdivision h_N :

$$0 = x_0 < x_1 < \dots < x_{N-2} < x_{N-1} = 1 \quad (5)$$

and the P_1 -Galerkin interpolation $\Pi_{h_N} u$ of u on this subdivision :

$$\begin{aligned} & \text{For } x_i \leq x \leq x_{i+1} : \\ & \Pi_{h_N} u(x) = \alpha u(x_i) + (1 - \alpha)u(x_{i+1}) \\ & \text{where : } \alpha = \frac{x - x_{i+1}}{x_i - x_{i+1}} \end{aligned} \quad (6)$$

2 Actual Convergence : soon capture property

2.1 Behaviour of the uniform-mesh strategy

The P_1 -continuous interpolation is known to be a second-order accurate one for the L^2 norm. This means that a twice finer mesh gives a four times smaller norm. Unfortunately, this occurs only when the mesh is fine enough to capture the smaller detail of the function u to be interpolated, and only if u is regular enough. We illustrate these remarks by the following measures :

- A series of uniform meshes \mathcal{M}_N is considered where N is the number of points.
- The four following functions u are considered.

$$u_1 = - \text{sign} \left(x - \frac{1}{2} \right) \quad (7)$$

$$u_2 = 1 - \frac{e^{\frac{2x}{\lambda}} - 1}{-1 + e^{\frac{1}{\lambda}}}, \quad \text{for } x < .5$$

$$u_2 = -1 + \frac{e^{\frac{-2x+1}{\lambda}} - 1}{e^{\frac{1}{\lambda}} - 1} \quad \text{for } x > .5 \quad (8)$$

$$u_2 = 0, \quad \text{for } x = .5$$

with $\lambda = .005$

$$u_3 = x - \frac{e^{\frac{x}{\lambda}} - 1}{e^{\frac{1}{\lambda}} - 1}, \quad \text{with } \lambda = .005 \quad (9)$$

$$u_4 = \sqrt{\left| x - \frac{1}{2} \right|} \quad (10)$$

Note that u_2 is a regularized version of u_1 . These solutions are sketched in Figure 1 ; u_2 and u_3 are smooth, u_1 is discontinuous, u_4 is continuous with a non bounded derivative.

The behavior of the usual linear interpolation L_2 error for $\|\Pi_h u - u\|_{L^2}$ for uniform meshes as a function of the N nodes used is depicted in Figures 2, 3, 4, 5 for the three above examples (solid lines) ; we observe that :

- First-order accuracy is showed initially by the regular cases u_2 and u_3 , and after the "investment" of about 100 nodes, second-order convergence appears ; if at most 30 nodes are used the scheme behaves just as a first-order accurate one.
- The two other test cases show first-order accuracy, for any mesh fineness.

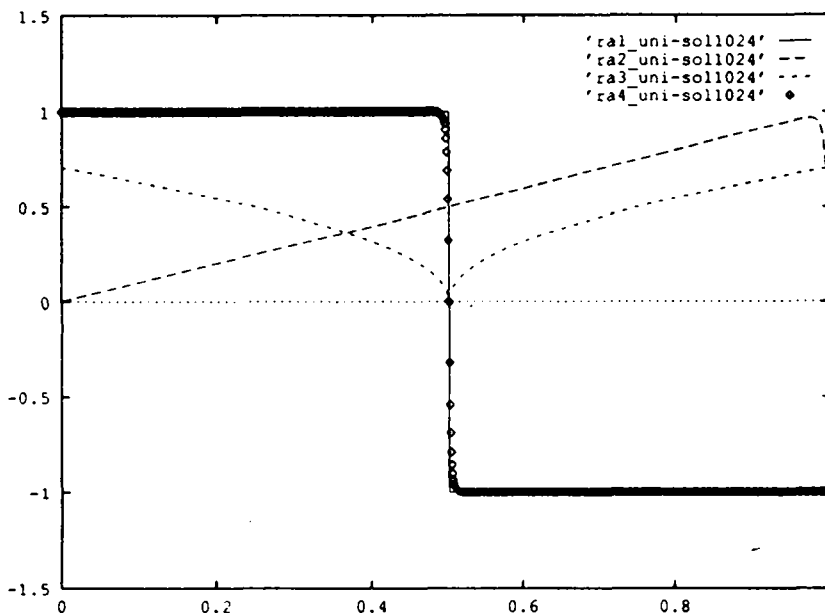


Figure 1 : Functions to be interpolated (—) u_1 , (. . .) u_2 ,
 (- - -) u_3 , (- . -) u_4 .

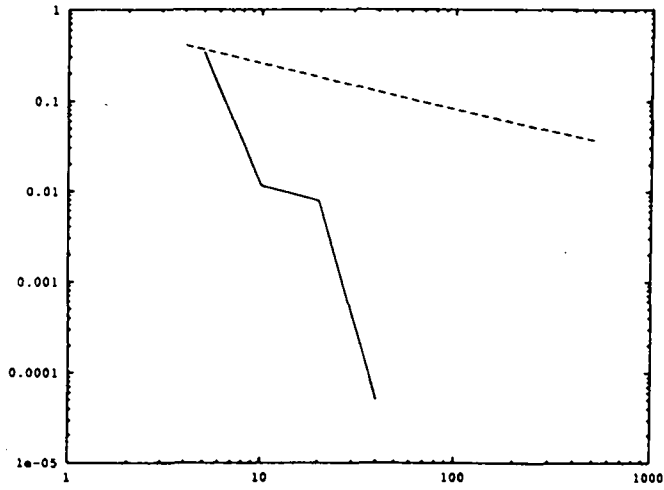


Figure 2 : Error analysis for u_1 :
 $\|u_1 - \Pi_h u_1\|_{L^2(0,1)}$ as a function of the number of nodes,
 (- - -) uniform mesh, (—) adapted.

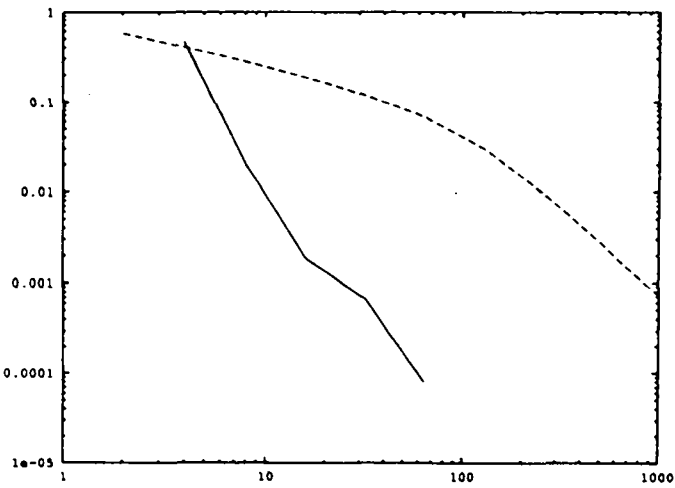


Figure 3 : Error analysis for u_2 :
 $\|u_2 - \Pi_h u_2\|_{L^2(0,1)}$ as a function of the number of nodes,
 (- - -) uniform mesh, (—) adapted.

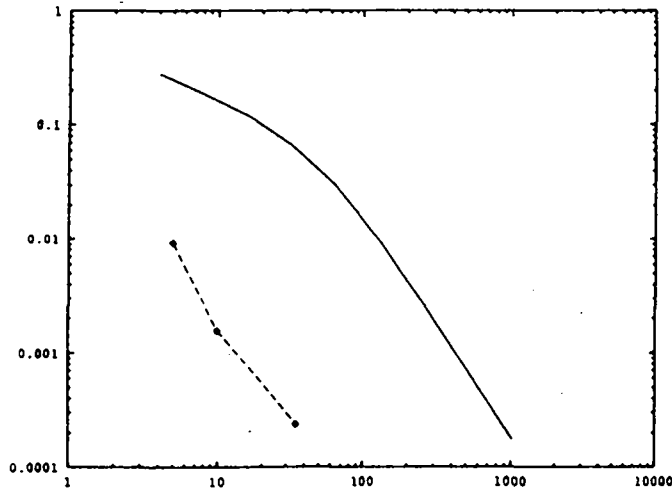


Figure 4 : Error analysis for u_3 :
 $\|u_3 - \Pi_h u_3\|_{L^2(0,1)}$ as a function of the number of nodes,
 (—) uniform mesh, (- - -) adapted.

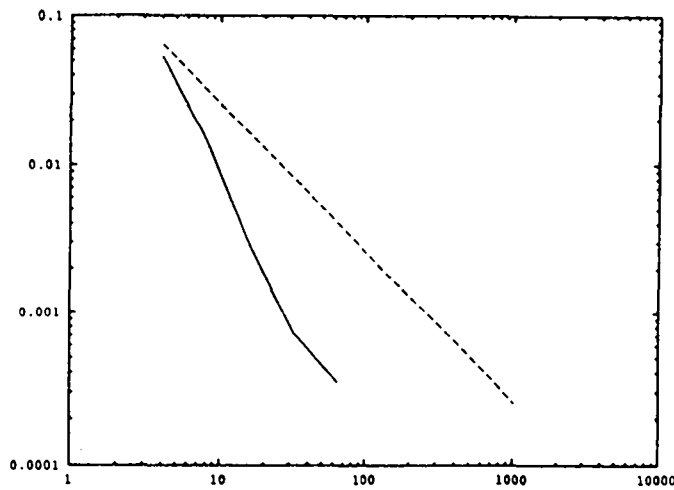


Figure 5 : Error analysis for u_4 :
 $\|u_4 - \Pi_h u_4\|_{L^2(0,1)}$ as a function of the number of nodes,
 (- - -) uniform mesh, (—) adapted.

2.2 A theoretical standpoint

We concentrate on the discontinuous case (like u_1). We want to prove that second-order accuracy can be obtained with a mesh adaptive strategy. Let us consider that u , defined on an interval $[0, 1]$, regular in $[0, 1]$ except in a point I , where it is discontinuous. Given a mesh subdivision of $[0, 1]$ with N nodes, let us call V a neighbour of I , V' its complementary in $[0, 1]$. The following estimates are hold:

$$\begin{aligned} \exists C \in R \\ \varepsilon_h &= \|\Pi_h u - u\|_{L^2(V)} \sim C/N \end{aligned} \quad (11)$$

$$\varepsilon'_h = \|\Pi_h u - u\|_{L^2(V')} \sim C/N^2 \quad (12)$$

If we use an adequate adaptive strategy, we obtain the following result:

Lemma 2.1: When multiplying by two the number of mesh subintervals in V' and by four the number of mesh subintervals in V , the L^2 norm $\|\Pi_h u - u\|_{L^2([0,1])}^$ on the refined mesh and the L^2 norm $\|\Pi_h u - u\|_{L^2([0,1])}^*$ on the initial mesh are related by:*

$$\|\Pi_h u - u\|_{L^2([0,1])}^* \sim 1/4 \|\Pi_h u - u\|_{L^2([0,1])}. \quad (13)$$

Thus, asymptotically:

$$\|\Pi_h u - u\|_{L^2([0,1])}^* = O(1/N^2) \quad (14)$$

This is the statement of the second order accuracy of $\|\Pi_h u - u\|_{L^2([0,1])}^$ extended to the case of an adaptive mesh.*

Proof of Lemma 2.1: When the number of nodes in V is multiplied by four, we note ε_h^* the L^2 norm $\|\Pi_h u - u\|_{L^2(V)}^*$ on the refined mesh in V and ε'_h the L^2 norm $\|\Pi_h u - u\|_{L^2(V')}^*$ on the refined mesh in V' and equation (12) becomes:

$$\varepsilon_h^* = \|\Pi_h u - u\|_{L^2(V)} \sim C/4.N \quad (15)$$

$$\varepsilon'_h = \|\Pi_h u - u\|_{L^2(V')} \sim C/(2.N)^2 = C/4.N^2. \quad (16)$$

Finally, we obtain:

$$\begin{aligned} \|\Pi_h u - u\|_{L^2([0,1])}^*{}^2 &= \|\Pi_h u - u\|_{L^2(V)}^*{}^2 + \|\Pi_h u - u\|_{L^2(V')}^*{}^2 \\ &\sim \frac{1}{16} (\varepsilon_h^2 + \varepsilon_h'^2) \end{aligned} \quad (17)$$

$$\begin{aligned} \|\Pi_h u - u\|_{L^2([0,1])}^*{}^2 &\sim \frac{1}{16} (\varepsilon_h^2 + \varepsilon_h'^2) \\ &= \frac{1}{16} \|\Pi_h u - u\|_{L^2([0,1])}^2 \end{aligned} \quad (18)$$

2.3 An example of mesh adaptive method

2.3.1 Definition of the method

Spring analogy in the 1 D context

We have extended the main idea that was applied by Gnoffo in [3], in the context of structured meshes to the case of unstructured meshes(see [6]). Each node is assumed to be connected to each neighbour (two nodes are said to be neighbours if they have a common edge) by an attractive strength corresponding to a fictitious spring: more precisely, the fictitious spring force applied to the node i and coming from the node j is:

$$\vec{F}_{i,j} = k_{i,j} \vec{i}j, \quad k_{i,j} \geq 0 \quad (19)$$

in which $k_{i,j}$ is the spring stiffness, while an opposed force is applied to the node j :

$$\begin{aligned} \vec{F}_{j,i} &= k_{j,i} \vec{j}i \\ k_{j,i} &= k_{i,j}. \end{aligned} \quad (20)$$

$k_{i,j}$ depends on the solution properties (for adaption). The unknowns are the coordinates $x(i)$ of vertices ($i = 1, \dots, N$, N is the number of vertices). The resulting mesh is the solution of the equilibrium system, which is written, for each vertex i :

$$\sum_{j \text{ neighbour of } i} \vec{F}_{i,j} = 0. \quad (21)$$

In the one dimensional case, each vertex i has only two neighbours $i - 1$ and $i + 1$. The mesh can be adapted in order to have a better representation of some sensor S , that is assumed to be numerically defined on each vertex i ; in short, we can put, for two adjacent nodes i, j :

$$k_{i,j} = \frac{|S(i) - S(j)|}{|x_i - x_j|} \quad (22)$$

which approximates the directional variation of the sensor S . In fact, a smoother value of the constant $k_{i,j}$ has to be introduced to take into account values at neighbours of nodes i and j , and to improve the computation; in the one dimensional case, $k_{i,i+1}$ is replaced by the following mean value (see [5]):

$$\frac{|\Delta_1| + |\Delta_2| + |\Delta_3|}{3} + \epsilon \quad (23)$$

with

$$\begin{aligned}
\Delta_1 &= \frac{S(i) - S(i-1)}{x_i - x_{i-1}} \\
\Delta_2 &= \frac{S(i+1) - S(i)}{x_{i+1} - x_i} \\
\Delta_3 &= \frac{S(i-1) - S(i-2)}{x_{i-1} - x_{i-2}} \\
\epsilon &= 1.D - 10
\end{aligned} \tag{24}$$

ϵ is a small constant added to assume the mesh system is well posed.

Mesh adaptive interpolation loop

In the mesh adaptive interpolation loop we choose the sensor S equal to the **exact interpolation of u** on each iterated mesh. The coupling between mesh and exact interpolation is obtained by converging to a fixed state the following loop:

- *interpolate u values on each node i ,*
- *compute the spring stiffness $k_{i,j}$,*
- *solve the mesh system.*

We refer to [5], [6], [7], for further details above the extension to MAA of this MAI algorithm.

2.3.2 Discussion of the $O(2)$ accuracy in a neighbour of a discontinuity

An illustration of the above theory is the possibility in discriminating truly second-order mesh adaptive methods; we give now an example.

Let us consider an 1-D spring mesh system: the locations x_i of the nodes are solutions of the following *spring equilibrium* system:

$$\left(\frac{|u_{i+1} - u_i|}{|x_{i+1} - x_i|^\alpha} + C \right) (x_{i+1} - x_i) = K, \tag{25}$$

where C is a small constant avoiding vanishing spring strength and K is a constant independant of i . We apply this system to a Heaviside function changing its value at $x = 0.5$ (function u_1 of Section 2); we denote by Δx_{jump} the size of the interval $[x_{i^*-1}, x_{i^*}]$ which contains two different values of the Heaviside function:

$$u_{i^*+1} - u_{i^*} = [u]_{jump} \neq 0. \tag{26}$$

We can write (26) for the jump and for the other intervals:

$$\left(\frac{[u]_{jump}}{(x_{i^*+1} - x_{i^*})^\alpha} + C\right)(x_{i^*+1} - x_{i^*}) = C(x_{i+1} - x_i), \forall i \neq i^*, \quad (27)$$

that we write, in short:

$$\left(\frac{[u]_{jump}}{\Delta x_{jump}^\alpha} + C\right)\Delta x_{jump} = C\Delta x_{const.} \quad (28)$$

Assuming that

$$\Delta x_{jump} = o(\Delta x_{const.}), \quad (29)$$

that can be possible if $\alpha > 0$, we get

$$\Delta x_{const.} = 0(1/N), \quad (30)$$

the equation (29) gives:

$$\Delta x_{const.} = 0(1/N^{\frac{1}{1-\alpha}}), \quad (31)$$

(for $\alpha \geq 1$ and N large (29) has no solution).

We observe that *a necessary and sufficient condition for having a capture of the discontinuity with n -order accuracy is:*

$$1 - 1/n \leq \alpha < 1. \quad (32)$$

This result extends to piecewise smooth functions.

2.3.3 Application of the MAA method to the functions (7), (8), (9), (10)

Applying the above Mesh Adaptive Interpolation algorithm appears to be able :

- to provide second-order convergence as soon as a very few nodes are invested (Figures 3, 4),
- to provide second-order convergence even for non regular functions (Figures 2, 5).

3 Second Idea : Frequency Analysis

3.1 Method

We recall a well-known mesh convergence test for spectral methods (see e.g. [3]) : when we apply a Chebyshev approximation to a given problem, the coefficient of the polynomials decreases with the polynomial number ; when the n -th coefficient is at zero machine, it is decided that a maximum practical accuracy is attained and that no extra polynomial is needed.

In the case of a one-dimensional uniform finite-element mesh, it is also possible to apply this kind of strategy : we can construct a sequence of finite-element basis functions with a decreasing mesh size : we construct embedded meshes with $N_p, N_{p-1}, N_{p-2}, \dots$ nodes:

$$N_p = 2^p + 1 \quad (33)$$

Denoting by Π_{N_p} the usual Lagrange P_1 -interpolation on the mesh with N_p nodes, we can develop the interpolation u_{N_p} as follows :

$$\begin{aligned} u &= \sum_{1 \leq k} \left(\Pi_{N_k} u - \Pi_{N_{k-1}} u \right), \\ \Pi_{N_0} u &= 0 \end{aligned} \quad (34)$$

$$\begin{aligned} u_{N_p} &= \sum_{1 \leq k \leq p} \left(\Pi_{N_k} u - \Pi_{N_{k-1}} u \right), \\ \Pi_{N_0} u &= 0 \end{aligned} \quad (35)$$

Note that the condition

$$\Pi_{N_0} u = 0 \quad (36)$$

is introduced by convention in the equations (29), (30), to obtain a simple general expression. The k -th frequential component $D_k u$ of u is defined as follows:

$$D_k u = u^k = \Pi_{N_k} u - \Pi_{N_{k-1}} u. \quad (37)$$

(note the analogy with hierarchical bases in finite elements).

For the sake of simplicity, we note:

$$\Pi_{N_k} u = \Pi_k u. \quad (38)$$

Note, by using (28),(29), (30), that:

$$u_{N_k} = \Pi_k u. \quad (39)$$

These components can be measured in L^2 -norm in function of k .

We present in Figures 7 to 10 a comparison of u^k in the case of a uniform mesh (1025 nodes) and an adapted one (65 nodes), for the functions $u_1 \dots u_4$ introduced in Section 2.

Since the series (28) should be of bounded sum, we have to examine the way the last terms go to zero.

We observe in Figures 7 to 10 that “interpolation convergence” arises with a much smaller number of nodes in the case of an adapted mesh ; again a phenomenon related to “soon capture” is noted, with a first erratic phase and then a linear convergence for “high frequencies”.

3.2 Theory

3.2.1 Existence and evaluation of an asymptotic slope

The observation of an asymptotic slope in frequency curves rises the question of the value of this slope and whether this slope is given by the order of interpolation. Some elements of (positive) answer are brought in the following lemmas, for which the assumption of embedded meshes (27) is essential.

Lemma 3.1: If

$$\|\Pi_k u - u\|_{L^\infty} = O(1/2^{k\alpha}), \quad \alpha = 2, \quad (40)$$

(respectively

$$\|\Pi_k u - u\|_{L^2} = O(1/2^{k\alpha}), \quad \alpha = 2,) \quad (41)$$

then, asymptotically,

$$\|D_k u\|_{L^\infty} = O(1/2^{k\alpha}). \quad (42)$$

(respectively

$$\|D_k u\|_{L^2} = O(1/2^{k\alpha}).) \quad (43)$$

Lemma 3.2: If

$$\|\Pi_k u - u\|_{L^\infty} = O(1/2^{k\alpha}), \quad \alpha = 2, \quad (44)$$

(respectively

$$\|\Pi_k u - u\|_{L^2} = O(1/2^{k\alpha}), \quad \alpha = 2, \quad (45)$$

and

$$\|D_k u\|_{L^\infty} = O(1/2^{k\beta}), \quad (46)$$

(and respectively

$$\|D_k u\|_{L^2} = O(1/2^{k\beta}), \quad (47)$$

then $\beta = \alpha$.

Remark that *Lemmas* 3.1 and 3.2 indicate that $\|D_k u\|$ and $\|\Pi_k u - u\|$ have the same asymptotic behaviour. The proof of *Lemma* 3.1 is the following:

$$|D_k u| = |\Pi_k u - \Pi_{k-1} u| \quad (48)$$

$$|D_k u| \leq |\Pi_k u - \Pi u| + |\Pi u - \Pi_{k-1} u| \quad (49)$$

So,

$$\begin{aligned} \|D_k u\|_{L^\infty} &\leq C/2^{k\alpha} + C/2^{(k-1)\alpha} \\ &= 5C/2^{k\alpha} \end{aligned} \quad (50)$$

then

$$\|D_k u\|_{L^\infty} = O(1/2^{k\alpha}). \quad (51)$$

Using L^2 norms, we easily obtain from (37) the required upper bound on $\|D_k u\|_{L^2}$:

$$\begin{aligned} \|D_k u\|_{L^2}^2 &\leq \|\Pi_k u - \Pi u\|_{L^2}^2 + \|\Pi u - \Pi_{k-1} u\|_{L^2}^2 \\ &\leq C'/2^{k\alpha}. \end{aligned} \quad (52)$$

Let us now turn to the proof of *Lemma* 3.2 in the case of L^∞ norms: The assumption $\beta < \alpha$ is in contradiction with the *Lemma* 3.1; with the assumption $\beta > \alpha$, we obtain:

$$\begin{aligned} \|\Pi_k u - u\|_{L^\infty} &\leq \sum_{l \geq k+1} \|D_l u\|_{L^\infty} \leq C(1/2^{(k+1)\beta} + 1/2^{(k+2)\beta} + \dots) \\ &\leq C/2^{(k+1)\beta}(1 + 1/2^\beta + \dots) \\ &\leq C'/2^{k\beta}. \end{aligned} \quad (53)$$

So, we obtain,

$$\|\Pi_k u - u\|_{L^\infty} = O(1/2^{k\beta}), \quad (54)$$

that is in contradiction with (34).

With L^2 norm, we obtain:

$$|\Pi_k u - u| \leq \sum_{l \geq k+1} |D_l u|. \quad (55)$$

Then

$$\|\Pi_k u - u\|_{L^2}^2 \leq 2 \sum_{l \geq k+1} \|D_l u\|_{L^2}^2 \geq C''/2^{k\beta}. \quad (56)$$

that is in contradiction with (28)

3.2.2 Evaluation of bounds for the L^2 interpolation error

A rather pleasant output of this analysis is that the behaviour and the size of the error can be estimated as far as we assume that the right part of the curve has the asymptotic behaviour:

Lemma 3.3 *If u is a concave function (respectively a convex function) that verifies:*

$$\|D_k u\|_{L^2} \sim C/2^\alpha, \quad (57)$$

with $\alpha = 2$

when the L^2 interpolation error $\|\Pi_k u - u\|_{L^2}$ lies asymptotically in the following interval:

$$[1/4 \|D_k u\|_{L^2}, 1/3 \|D_k u\|_{L^2}]. \quad (58)$$

Remark: the assumption (51) on $\|D_k u\|_{L^2}$ is verified with the functions introduced in Section 2.

Proof of *Lemma 3.3* in the case of a concave function u , upper bound:

$$|\Pi_k u - u| = \left| \sum_{l \geq k+1} D_l u \right| \leq \sum_{l \geq k+1} |D_l u|. \quad (59)$$

From *Lemma 3.1*, it becomes:

$$\sum_{l \geq k+1} |D_l u| \leq |D_{k+1} u| (1 + 1/4 + 1/4^2 + \dots) \quad (60)$$

$$\leq |D_{k+1} u| / (1 - 1/4) \quad (61)$$

$$\sum_{l \geq k+1} |D_l u| \leq 4/3 \cdot 1/4 |D_k| = 1/3 |D_k| \quad (62)$$

So

$$|\Pi_k u - u| \leq 1/3 |D_k u|. \quad (63)$$

and

$$\|\Pi_k u - u\|_{L^2} \leq 1/3 \|D_k u\|_{L^2}. \quad (64)$$

The proof of *Lemma 3.3*, upper bound does not use the assumption on u (concave or convex), so it is verified also if u is a convex function.

Proof of *Lemma 3.3* in the case of a concave function u , lower bound: If u is a concave function (see Figure 6), we obtain asymptotically:

$$D_k u = \Pi_k u - \Pi_{k-1} u \geq 0 \quad (65)$$

$$\sum_{l \geq k+1} D_l u \geq D_{k+1} u = |D_{k+1} u| \quad (66)$$

$$\left| \sum_{l \geq k+1} D_l u \right| = \sum_{l \geq k+1} D_l u \geq |D_{k+1} u| \quad (67)$$

$$|\Pi_k u - u| \geq |D_{k+1} u| \quad (68)$$

Then

$$\|\Pi_k u - u\|_{L^2} \geq \|D_{k+1} u\|_{L^2}. \quad (69)$$

Moreover,

$$\|D_{k+1}\|_{L^2} \sim 1/4 \|D_k u\|_{L^2}. \quad (70)$$

So, asymptotically,

$$\|\Pi_k u - u\|_{L^2} \geq 1/4 \|D_k u\|_{L^2}. \quad (71)$$

Proof of *Lemma 3.3* in the case of a convex function u , lower bound: Remarking that:

$$\|D_k u\| = \|-D_k u\| \quad (72)$$

and that if u is a convex function, $-u$ is a concave function, we apply the previous proof to the function $-u$.

Note that the concavity of u is only used for the lower bound estimate.

3.2.3 Extension to general functions

Let us recall $(0, 1)$ the interval of integration for the L^2 norms. Let us call $(*)$ the following assumption on u :

$(*)$: u is a function that is either concave either convex, except in a finite number points p_1, p_2, \dots, p_m of $(0, 1)$.

We note Conc (resp. Conv) the part of $(0, 1)$ on what u is concave (resp. convex) and I_1, I_2, \dots, I_m small intervalls containing p_1, p_2, \dots, p_m .

So we have:

$$(0, 1) = Conc \cup Conv \cup I_1 \cup I_2 \cup \dots \cup I_m. \quad (73)$$

Lemma 3.5 *Lemma 3.3 holds also if u is a function verifying assumption (*)*.

Proof of the lower bound:

$$\|\Pi_k u - u\|_{L^2}^2 = \int_a^b \sum_{l \geq k+1} D_l u^2 dx. \quad (74)$$

$$\int_a^b \sum_{l \geq k+1} D_l u^2 dx = \int_{Conv} \sum_{l \geq k+1} D_l u^2 dx + \int_{Conc} \sum_{l \geq k+1} D_l u^2 dx + \int_{I_1 \cup I_2 \cup \dots \cup I_m} D_l u^2 dx. \quad (75)$$

$$\|\Pi_k u - u\|_{L^2} \geq \int_{Conv} \sum_{l \geq k+1} D_l u^2 dx + \int_{Conc} \sum_{l \geq k+1} D_l u^2 dx. \quad (76)$$

From Lemmas 3.4, 3.5, we deduce:

$$\int_{Conv} \sum_{l \geq k+1} D_l u^2 dx \geq 1/16 \int_{Conv} D_k u^2 dx, \quad (77)$$

$$\int_{Conc} \sum_{l \geq k+1} D_l u^2 dx \geq 1/16 \int_{Conv} D_k u^2 dx. \quad (78)$$

Finally, we obtain:

$$\|\Pi_h u - u\|_{L^2}^2 \geq 1/16 \|D_k u\|_{L^2}^2 - 1/16 \int_{I_1 \cup I_2 \cup \dots \cup I_m} \sum_{l \geq k+1} D_l u^2 dx \quad (79)$$

$$\int_{I_1 \cup I_2 \cup \dots \cup I_m} \sum_{l \geq k+1} D_l u^2 dx = \int_{I_1 \cup I_2 \cup \dots \cup I_m} \chi \sum_{l \geq k+1} D_l u^2 dx \leq \|\chi\|_{L^2}^2 \left\| \sum_{l \geq k+1} D_l u \right\|_{L^2}^2, \quad (80)$$

where χ is the characteristic function of

$$I_1 \cup I_2 \cup \dots \cup I_m. \quad (81)$$

$$\int_{I_1 \cup I_2 \cup \dots \cup I_m} \sum_{l \geq k+1} D_l u^2 dx \leq 1/16 \|\chi\|^2 \|D_k u\|_{L^2}^2 \quad (82)$$

$\|\chi\|_{L^2}$ can be chosen as small as we want. So, for all $\epsilon > 0$ and for $k \geq k_0$, there exist I_1, I_2, I_m such that:

$$\|\chi\|_{L^2} \leq 3\epsilon/\|D_k u\|_{L^2}. \quad (83)$$

Then, for $k \geq k_0$

$$\|\Pi_k u - u\|_{L^2}^2 \geq 1/16\|D_k u\|_{L^2}^2 - \epsilon^2 \quad (84)$$

So, asymptotically,

$$\|\Pi_k u - u\|_{L^2} \geq 1/4\|D_k u\|_{L^2} \quad (85)$$

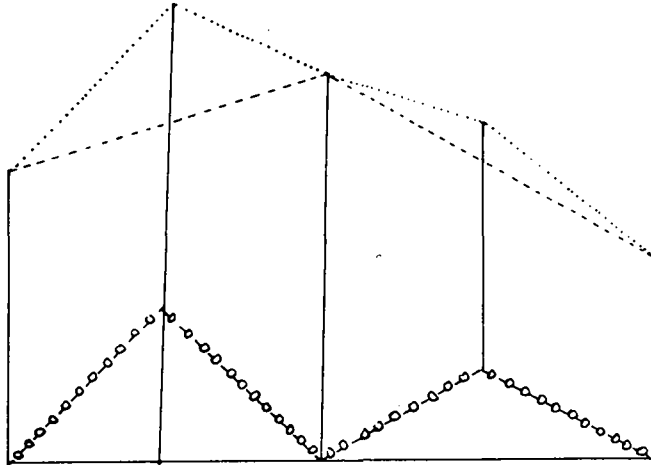


Figure 6 : Nested P1 Galerkin interpolation,
in the case of concave function u , (--) $\Pi_k u$, (..) $\Pi_{k-1} u$, (-o-) $D_k u$.

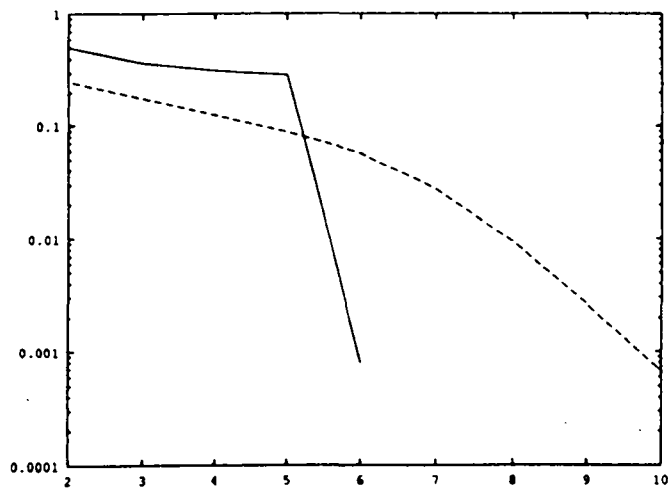


Figure 7 : Frequency analysis for u_1 :
 L_2 norm of u_1 as a function of the level p of the mesh, $N_p = 2^p + 1$;
 (- - -) uniform 1025 nodes
 (—) adapted, 65 nodes

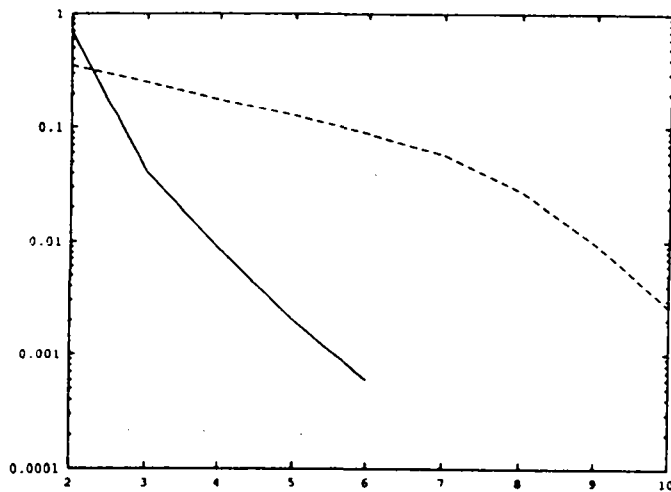


Figure 8 : Frequency analysis for u_2 :
 L_2 norm of u_2 as a function of the level p of the mesh, $N_p = 2^p + 1$;
 (- - -) uniform 1025 nodes
 (—) adapted, 65 nodes

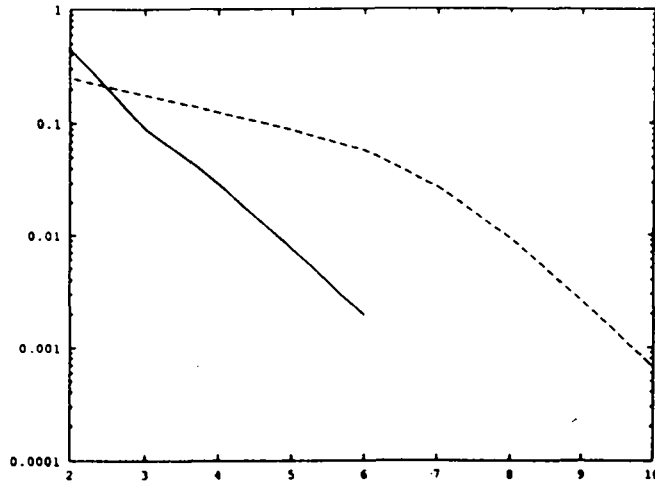


Figure 9 : Frequency analysis for u_3 :

L_2 norm of u_3 as a function of the level p of the mesh, $N_p = 2^p + 1$;

(- - -) uniform 1025 nodes

(—) adapted, 65 nodes

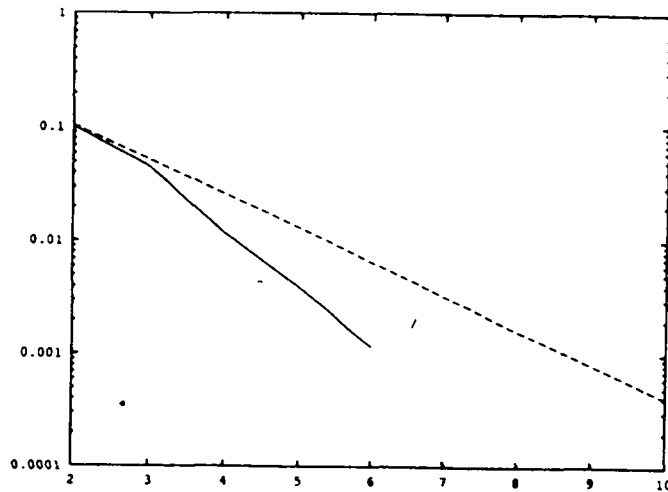


Figure 10 : Frequency analysis for u_4 :

L_2 norm of u_4 as a function of the level p of the mesh, $N_p = 2^p + 1$;

(- - -) uniform 1025 nodes

(—) adapted, 65 nodes

3.3 Numerical illustration

We use the above functions for illustrating the accuracy of this estimate, the results are depicted in Table 2.

CASE	$\ D_k u\ _{L^2}$	$1/4 \ D_k u\ _{L^2}$	$\ \Pi_k u - u\ _{L^2}$	$1/3 \ D_k u\ _{L^2}$
Case 2: uniform	$1.9 \cdot 10^{-4}$	$4.7 \cdot 10^{-4}$	$4.9 \cdot 10^{-4}$	$6.3 \cdot 10^{-4}$
Case 2: adaptive	$6.7 \cdot 10^{-4}$	$1.67 \cdot 10^{-4}$	$1.7 \cdot 10^{-4}$	$2.2 \cdot 10^{-4}$
Case 3: adaptive	$11 \cdot 10^{-4}$	$2.7 \cdot 10^{-4}$	$3.2 \cdot 10^{-4}$	$3.6 \cdot 10^{-4}$
Case 4: uniform	$2.59 \cdot 10^{-3}$	$6.5 \cdot 10^{-4}$	$6.9 \cdot 10^{-4}$	$8.7 \cdot 10^{-4}$
Case 4: adaptive	$5.94 \cdot 10^{-4}$	$1.48 \cdot 10^{-4}$	$1.53 \cdot 10^{-4}$	$1.98 \cdot 10^{-4}$

Table 2 : Numerical illustration of the accuracy in the a priori error interval (columns 2 and 4), to be compared with the measured error, column 3.

4 Some Concluding remarks

We have proposed a deeper examination of the convergence behaviour of interpolations towards a function when non uniform meshes are applied.

The phenomenon called “soon capturing” is observed (and in some cases theoretically predicted) in the two contexts of adaptive mesh convergence and frequency analysis; in particular, the estimation of the lower and upper bounds of the L^2 error seems of particular interest.

The 1-D results are encouraging, and could already be applied to practical problems like turbulent boundary layers, see [2].

In the near future, we shall examine the extension to 2-D case of the two above analyses.

Extension to multidimensional unstructured case needs new ideas for building a intelligent coarsening in the case of non-structured meshes, a very challenging theme for mesh adaption purpose; we refer to [1] for advances in this field.

Yet, the correlation between mesh adaptive interpolation and mesh adaptive PDE approximation remains to be well understood.

5 References

- [1] ABGRALL R., HARTEN A., *Multiresolution Representation in Unstructured Meshes : I. preliminary report*, UCLA CAM, 94-20, 1994.
- [2] CARRAU A., DERVIEUX A., *Application of a mesh adaptive capture strategy for solving 1D turbulent boundary layers*, Proceedings of the 4th international conference on numerical grid generation in computational fluid dynamics and related topics, N.-P. Weatherill and P.-R. Eiseman and J. Hauser and J.-F. Thompson Editor, Pineridge Press Ltd., Swansea, Wales, pp 513-526, 6-8 Avril, 1994.
- [3] GNOFFO P.A., *A finite volume adaptive grid algorithm applied to planetary entry flowfields*, *AIAA J.* **21**, 1249-1254 (1983).
- [4] GUILLARD H., PEYRET R., *On the use of spectral methods for numerical solution to stiff problems*. *Comput. Methods in Appl. Mech. Eng.* 66,17, 1988.
- [5] PALMERIO B., *A Two Dimensional F.E.M. Adaptive Moving Node Method for Steady Euler Flow Simulation*, *Computer Methods in Applied Mechanics and Engineering* 71 (1988) 315-340.
- [6] PALMERIO B., *An Attraction-Repulsion Mesh Adaptation Model For Flow Solution On Unstructured Grids*, *Computers and Fluids* Vol. 23, No. 3 (487-506), 1994.
- [7] PALMERIO B., DERVIEUX A., *On Weak and Strong Coupling Between Mesh Adaptors and Flow Solvers*, 12th International Conference on numerical methods in Fluid Dynamics, University of Oxford, Jul. 9-13, 1990, *Lecture Notes in Physics* 371, 540-544, 1990. K.W. Morton ed., Springer Verlag.
- [8] DERVIEUX A., PALMERIO B., *Advances In Mesh Adaptation For CFD*, The 5th International Symposium On Refined Flow Modelling and Turbulence Measurements, september 7-10 (1993), Paris.
- [9] PALMERIO B., DERVIEUX A., *Mesh Adaptive Interpolation: Towards a Mini Theory?*, 4th International Conference in Numerical Grid Generation in Computational Fluid Dynamics and Related Fields, Swansea, 6-8 april 1994, UK.



Unité de recherche INRIA Sophia Antipolis
2004, route des Lucioles - B.P. 93 - 06902 Sophia Antipolis Cedex (France)

Unité de recherche INRIA Lorraine - Technopôle de Nancy-Brabois - Campus scientifique
615, rue du Jardin Botanique - B.P. 101 - 54602 Villers lès Nancy Cedex (France)
Unité de recherche INRIA Rennes - IRISA, Campus Universitaire de Beaulieu 35042 Rennes Cedex (France)
Unité de recherche INRIA Rhône-Alpes - 46, avenue Félix Viallet - 38031 Grenoble Cedex 1 (France)
Unité de recherche INRIA Rocquencourt - Domaine de Voluceau - Rocquencourt - B.P. 105 - 78153 Le Chesnay Cedex (France)

Éditeur
INRIA - Domaine de Voluceau - Rocquencourt - B.P. 105 - 78153 Le Chesnay Cedex (France)

-ISSN 0249 - 6399



★ R R - 2 7 2 2 ★